An Efficient Switching Algorithm for the Implementation of Synchronous Space Vector Modulation for an Induction Motor Drive with (V/f) Control

K.A.S. Mallikarjuna Rao[1] Sunita Nadampalli[2] V.T. Somasekhar[3]

Abstract – In this paper, an improvisation to an existing switching algorithm is described for the implementation of synchronized space vector modulation for a 3-phase, 2-level VSI driven induction motor with V/f control. A useful corollary is derived for this specific situation from an existing general algorithm. This corollary considerably alleviates the computational burden on the digital controller. The reduction of the computational time to determine the switching times of individual phases of the inverter is obtained by employing an appropriately devised lookup table. The elegance of the improvised algorithm lies in the fact that the elements of the lookup table could be employed for any modulation index, when the inverter is operated in the region of linear modulation. The proposed algorithm is experimentally implemented on a TMS 320F243 DSP platform and the results are presented.

Keywords – Two-level inverter, space vector modulation, induction motor drive, V/f control, effective time.

I. INTRODUCTION

Figure 1 shows a 3-phase, 2-level voltage source inverter (VSI). Owing to its simplicity and ruggedness, it has become a natural choice in various AC drives. With the advancements in the Pulse Width Modulated (PWM) control schemes, the harmonic spectrum of the output voltage can be maneuvered to contain a pronounced fundamental component and to transfer the harmonic energy to the components of higher frequency. This is desirable, as it is relatively easier to filter out the components of higher frequency.

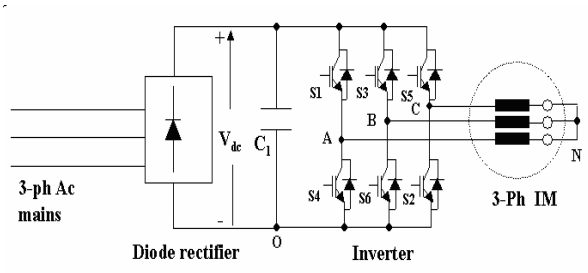

Fig.1: A conventional Induction motor drive with 2-level inverter

The paper first received 22 Feb 2007 and in revised form 23 Mar 2007.
Digital ref: AI70301155

[1] Senior Engineer, Ashok Leyland Ltd., Chennai, India

[2] Software Design Engineer, Texas Instruments (India) Ltd., Bangalore, India, E-mail: sunitan@ti.com

[3] Assistant Professor, Department of Electrical Engineering, National Institute of Technology, Warangal, India, E-mail: vtsomasekhar@rediffmail.com

Several PWM scheme are reported in the literature [1-12], of which the sine-triangle PWM (SPWM) and the space vector modulation (SVM) have aroused a particular interest in academia as well as in practicing engineers. Of these two modulation schemes, SVM yields a superior spectral performance [4]. Also SVM enhances the DC bus utilization by about 15% compared to SPWM [4]. Several methods to implement SVM are reported in the literature.

In SVM, the instantaneous reference phase voltages (denoted as v_a^*, v_b^* and v_c^*) are converted into a corresponding space vector v_{sr} defined as:

$$v_{sr} = v_a^* + v_b^* e^{j2\pi/3} + v_c^* e^{-2\pi/3} \quad (1)$$

The reference space vector v_{sr} is expressed in rectangular form as:

$$v_{sr} = v_\alpha + jv_\beta \quad (2)$$

It is expressed in the polar form as:

$$v_{sr} = |v_{sr}| \angle \theta \quad (3)$$

where

$$|v_{sr}| = \sqrt{v_\alpha^2 + v_\beta^2} \text{ and } \theta = \tan^{-1}\left(\frac{v_\beta}{v_\alpha}\right) \quad (4)$$

The quantities v_{sr} , v_α , v_β and θ are shown in Fig 2. A three phase, 2-level VSI is capable of assuming 8 states. Of these, six states allow power transfer from the DC-link to AC side. Hence they are called the active states. The other two states are termed as null states, as all the three phases on the AC side are short circuited either to the positive bus or to the negative bus. Consequently, there is no power flow from the DC-link to the AC side. The null vectors are located at the center of the hexagon. The switching states corresponding to each vertex are also shown in Fig.2. For example, the state-1 is identified as (+ - -). This means that for this state the top switch in phase-A leg (S_1 in Fig.1) is turned on so that the output terminal of phase-A is connected to the positive bus of the DC-link. Similarly, the phase-B and phase-C terminals are connected to the negative bus of the DC-link by turning on the switches S_6 and S_2 in state '1'. From Fig..2 it is evident that the hexagon is subdivided into six identical sectors. The central theme of SVM is to synthesize the reference voltage space vector v_{sr} in the average sense with the eight states offered by the inverter, using the criterion of volt-second balance.

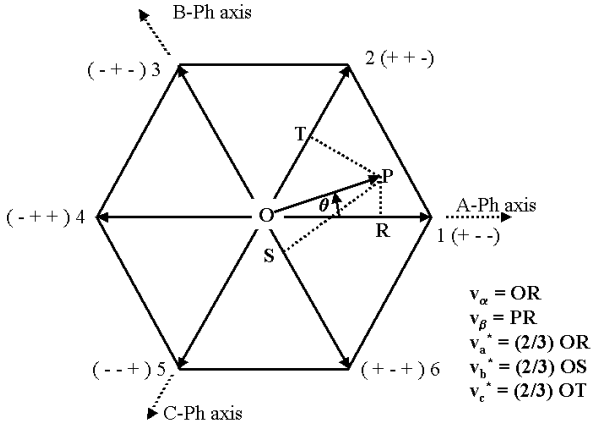

Fig. 2: Space vector diagram of a 3-ph, 2-level inverter

To this end, the instantaneous reference phase voltages are sampled at regular intervals. The sampling time period is denoted as T_s. The modulation index, denoted as m_i, is defined as:

$$m_i = \frac{|v_{sr}|}{V_{dc}}$$

where V_{dc} is the DC-link voltage.

The time intervals T_{ga}, T_{gb} and T_{gc} respectively denote the time periods for which the corresponding phase terminal is connected to the positive bus. For the rest of the paper, they are referred as the 'inverter-leg switching time periods'.

In conventional method of implementing SVM, the sector in which the tip of the reference space vector is situated is first determined. Using the criterion of the volt-second balance, the periods corresponding to the switching of the active vectors along the leading edge (denoted as T_1 and T_2 respectively) of that sector during that sampling time period are then determined [4]. There exists an exclusive relationship between the active vector switching time periods (T_1 and T_2) and the inverter leg switching time periods (T_{ga}, T_{gb} and T_{gc}) in a given sector. Using these relationships the time periods T_1 and T_2 are translated into the gating signals of the individual inverters. This method is thus cumbersome and time consuming. Reference [13] describes an elegant switching algorithm, which uses only instantaneous phase reference voltages to implement SVM. For the rest of this paper this algorithm is referred as the 'Kim-Sul, algorithm, in the honor of its inventors. In the following section, the Kim-Sul algorithm is briefly reviewed.

II. THE KIM-SUL ALGORITHM

As stated earlier, this algorithm operates only with the instantaneous reference voltages. The elegance of this algorithm lies in the fact that sector identification is not required to implement the SVM and the generation of gating signals is automatically accomplished.

In sector1, the switching periods for the active vectors T_1 and T_2 may be expressed in terms of the instantaneous values of the reference phase voltages v_a^*, v_b^* and v_c^* as [13]:

$$T_1 = \frac{T_s (v_a^* - v_b^*)}{V_{dc}}; \qquad T_2 = \frac{T_s (v_b^* - v_c^*)}{V_{dc}} \tag{5}$$

The switching time periods proportional to the instantaneous values of the reference phase voltages, termed imaginary switching times, are defined as [13]

$$T_{as} = \left(\frac{T_s}{V_{dc}}\right) v_a^*; T_{bs} = \left(\frac{T_s}{V_{dc}}\right) v_b^*; T_{cs} = \left(\frac{T_s}{V_{dc}}\right) v_c^* \tag{6}$$

From (1) and (2) the active vector switching times T_1 and T_2 in sector1 may be expressed as:

$$T_1 = T_{as} - T_{bs} \; ; \; T_2 = T_{bs} - T_{cs} \; ; \tag{7}$$

Extending this procedure for the other sectors, the active vector switching times T_1 and T_2 for the respective sectors may be expressed in terms of the imaginary switching times T_{as}, T_{bs} and T_{cs} for a particular sampling time period. The effective time T_{eff} is the time during which the active vectors are switched in a sector and is given by $(T_1 + T_2)$. This may be determined as the difference between the maximum and minimum values among T_{as}, T_{bs} and T_{cs}. The time duration T_o is the time for which a null vector is applied, may be obtained from T_1 and T_2 as:

$$T_o = T_s - (T_1 + T_2) = (T_s - T_{eff}) \tag{8}$$

where

$$\begin{aligned} T_{eff} &= \max\{T_{as}, T_{bs}, T_{cs}\} - \min\{T_{as}, T_{bs}, T_{cs}\} \\ &= T_{\max} - T_{\min} \end{aligned} \tag{9}$$

The offset time, T_{eff} required during a given sampling time period to distribute the null vector symmetrically at either end of the effective time period with half the duration $(T_o / 2)$ each (or place the effective time period exactly at the center of the sampling time period) is given by [13]:

$$T_{offset} = (T_o / 2) - T_{\min} \tag{10}$$

The actual switching times for each inverter leg can be obtained by the time shifting operation as follows:

$$\begin{aligned} &T_{ga} = T_{as} + T_{offset}; T_{gb} = T_{bs} + T_{offset} \\ &T_{gc} = T_{cs} + T_{offset} \end{aligned} \tag{11}$$

To achieve minimum switching, the vectors are switched in the sequence 8-1-2-7 with the time duration of $T_o/2 - T_1 - T_2 - T_o/2$ for one sampling time duration and in the sequence 7-2-1-8 during the next sampling time period, when tip of the reference vector is in sector 1. The former sequence is called the 'ON' sequence and the later sequence is called 'OFF' sequence. These two sequences are alternatively used. Since the time periods T_{gx} (x = a,b,c) denote the time duration for which a given phase is connected to the positive bus, transitions occur in the

respective phases after the time duration of T_{gx} from the beginning of the sampling time period for all the samples with 'OFF' sequence. However for the 'ON' sequence, transitions occur in respective phases after T'_{gx} (x = a,b,c) from the beginning of the sampling time period where

$T'_{gx} = T_s - T_{gx}$ (x = a,b,c)

The procedure outlined in the previous paragraphs is graphically depicted in Fig.3, assuming that the sample is situated in sector-1.

when the induction motor is operated with V/f control and the inverter is modulated with Synchronous SVM, the imaginary switching times remain the same in the range of linear modulation for various modulation indices. This is because:

- When the inverter is operated with Synchronized SVM, n_{sam} is constant.
- When the induction motor is operated with (V/f) control the quantities enclosed in braces namely

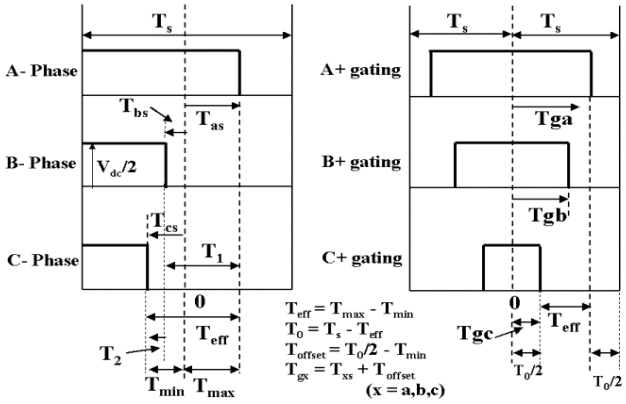

Fig. 3: Implementation of the space-phasor modulation scheme using the instantaneous values of the ref. phase voltages – v_a^*, v_b^* and v_c^*.

III. The Proposed Algorithm

A. *The Algorithm*

With synchronized PWM, a fixed number of samples are used for any fundamental frequency. This is achieved by making T_s as a variable. This would ensure that the location of the first sample of the previous cycle and the location of the first sample of the current cycle are exactly aligned. Assuming that the reference phase voltages are sampled n_{sam} times in the fundamental cycle which has a time period T,

$$T_s = \frac{T}{n_{sam}} = \frac{1}{f n_{sam}} \tag{12}$$

where f is the frequency of the fundamental component. A very useful simplification results if the inverter is operated with synchronized SVM and the induction motor is driven with V/f control. The expressions for the imaginary switching times T_{as}, T_{bs} and T_{cs} are reproduced below for an easy reference.

$$T_{as} = \left(\frac{T_s}{V_{dc}}\right) v_a^*; T_{bs} = \left(\frac{T_s}{V_{dc}}\right) v_b^*; T_{cs} = \left(\frac{T_s}{V_{dc}}\right) v_c^* \tag{13}$$

Substituting equ. (8) in equ. (9)

$$T_{as} = \left(\frac{1}{n_{sam} V_{dc}}\right)\left(\frac{v_a^*}{f}\right); T_{bs} = \left(\frac{1}{n_{sam} V_{dc}}\right)\left(\frac{v_b^*}{f}\right);$$

$$T_{cs} = \left(\frac{1}{n_{sam} V_{dc}}\right)\left(\frac{v_c^*}{f}\right) \tag{14}$$

(V_a^*/f), (V_b^*/f) and (V_c^*/f) remain constant irrespective of the modulation index in the range of linear-modulation. Hence for a given space angle of space vector θ, irrespective of the value of modulation index the following statements are true when the inverter is operated in the range of linear modulation:

- T_{as}, T_{bs} and T_{cs} are constant.
- $T_{\max}$ and $T_{\min}$, the maximum and minimum values among T_{as}, T_{bs} and T_{cs} respectively are constant. This observation is based on the fact that T_{as}, T_{bs} and T_{cs} are phase shifted by 120^0 with respect to each other as v_a^*, v_b^* and v_c^* are thus phase shifted.
- $T_{eff} = T_{\max} - T_{\min}$, the effective time is constant.

The above observations may be used to derive a useful corollary to simplify Kim-Sul algorithm.

According to Kim-Sul algorithm, T_o (Null state period) =

$T_s - T_{eff}$ and T_{offset} (Offset period) $= \frac{T_o}{2} - T_{\max}$

$$T_{offset} = \left(\frac{T_s - T_{eff}}{2}\right) - T_{\min} = \frac{T_s}{2} - \left(\frac{T_{\max} - T_{\min}}{2}\right) - T_{\min}$$

$$T_{offset} = \frac{T_s}{2} - \left(\frac{T_{\max} + T_{\min}}{2}\right) \tag{15}$$

Hence the inverter-leg switching time period for the A-phase i.e. T_{ga} is given by $T_{ga} = T_{as} + T_{offset}$ and the substitution of eqn.15 yields

$$T_{ga} = \frac{T_s}{2} + \left\{ T_{as} - \left(\frac{T_{\max} + T_{\min}}{2} \right) \right\} \tag{16}$$

Hence

$$T_{ga} = T_{const\_a} + \frac{T_s}{2} \tag{17}$$

for OFF sequence.

However, as explained in section-2, during the 'ON' sequence

$$T_{ga} = T_s - T_{ga} = T_{const\_a} - \frac{T_s}{2} \tag{18}$$

for ON sequence

where

$$T_{const\_a} = T_{as} - \left(\frac{T_{\max} + T_{\min}}{2} \right) \tag{19}$$

T_{const_a} is defined as that component of actual switching time (T_{ga}) that is independent of modulation index and only depends on space angle (θ) of space vector. Similarly, T_{const_b} and T_{const_c} are defined as that component of actual switching times (T_{gb} and T_{gc}) which are independent of modulation index and only depend on space angle (θ) of space vector.

B. Relation between T_{const_a}, T_{const_b} and T_{const_c}

As T_{as}, T_{bs} and T_{cs} are directly proportional to v_a^*, v_b^* and v_c^* respectively, T_{as}, T_{bs} and T_{cs} can be represented as three vectors which are displaced in phase by 120˚ with each other like v_a^*, v_b^* and v_c^*. From the Fig. 2 it is evident that, after affecting a phase shift of $\pm$120˚ or $\pm$240˚, the positions of vectors interchange among them. Hence, $T_{\max}$ and $T_{\min}$, which are defined as maximum and minimum among T_{as}, T_{bs} and T_{cs} remain constant after $\pm$120˚ and $\pm$240˚ of phase shift.

The above observation can be represented in equations as:

$$T_{\max}(120^0 + \theta) = T_{\max}(240^0 + \theta) = T_{\max}(\theta) \tag{20}$$

$$T_{\min}(120^0 + \theta) = T_{\min}(240^0 + \theta) = T_{\min}(\theta) \tag{21}$$

From Fig.4 it can be observed that

$$T_{bs}(\theta) = T_{as}(240^0 + \theta) \tag{22}$$

$$T_{cs}(\theta) = T_{as}(120^0 + \theta) \tag{23}$$

From equation (19)

$$T_{const\_a}(120^o + \theta) = T_{as}(120^0 + \theta) - [\{(T_{\max}(120^o + \theta) + T_{\min}(120^o + \theta)\}/2]$$

From equations (20), (21) and (23)

$$T_{const\_a}(120^o + \theta) = T_{cs}(\theta) - \{T_{\max}(\theta) + T_{\min}(\theta)\}/2 = T_{const\_c}(\theta) \tag{24}$$

From equation (19)

$$T_{const\_a}(240^o + \theta) = T_{as}(240^o + \theta) - (T_{\max}(240^o + \theta) + T_{\min}(240^o + \theta))/2$$

From equations (20), (21) and (22)
i.e.

$$T_{const\_a}(240^0 + \theta) = T_{bs}(\theta) - (T_{\max}(\theta) + T_{\min}(\theta))/2 = T_{const\_b}(\theta) \tag{25}$$

Hence T_{const_a}, T_{const_b} and T_{const_c} are phase shifted by 120˚. A variable T_{const} is defined as that component of actual switching time (T_{ga}), which is independent of modulation index and only depends on phase angle (θ) of space vector. Equations (26), (27) and (28) express T_{const_a}, T_{const_b} and T_{const_c} in terms of T_{const}.

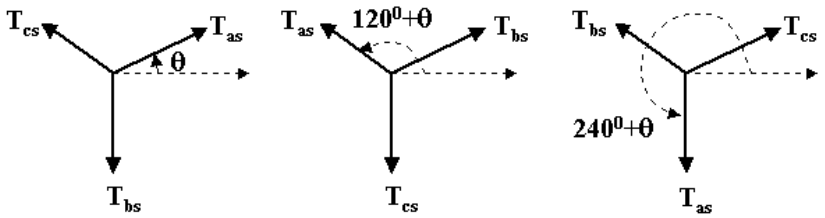

Fig. 4: Phasor diagram of T_{as}, T_{bs} and T_{cs}

$$T_{const\_a}(\theta) = T_{const}(\theta) \quad (26)$$

$$T_{const\_b}(\theta) = T_{const}(240^0 + \theta) \quad (27)$$

$$T_{const\_c}(\theta) = T_{const}(120^0 + \theta) \quad (28)$$

In synchronized SVM, the numbers of samples are constant irrespective of frequency. Hence the space angle 'θ' takes a fixed set of values. The values of T_{const} at those fixed values can be computed offline. By a simple addition or subtraction of the value of $\frac{T_s}{2}$ depending on the sequence to T_{const}, one can obtain actual switching time to a-phase. As actual switching times are phase shifted by 120º, actual switching times of the other two phases can also be determined.

From the above discussion, it is evident that the Kim-Sul algorithm can be further simplified when the inverter is operated with synchronized SVM and the induction motor with (V/f) control.

The Modified Kim-Sul algorithm can formally be stated as follows:

- Off-line calculation of T_{const} values of the output voltage at the prefixed values of θ and storing these values in the form of an array.
- Calculation of T_{ga} by simply adding $T_s/2$ to T_{const} for OFF sequence.
- Calculation of T_{ga} by simply subtracting $T_s/2$ from T_{const} for ON sequence.
- Calculation of T_{gb} and T_{gc} by accessing the elements from the T_{const} array, which are phase shifted by $(+240^0)$ and $(+120^0)$ respectively (Fig.4).

IV. Experimental Results and Discussion

A 3-ph, 2-level inverter controlled by the proposed algorithm has been implemented on a TMS320F243 DSP platform. A (V/f) controlled induction motor drive is considered for experimentation. The induction motor rating is 5HP, 415 V (line-line).

The time period of the fundamental component of the motor phase voltage is divided into 48 samples irrespective of the time period. This means that the angular difference between successive samples is 7.5^0 (i.e. $360^0/48$).

The radius of the biggest circle that can be inscribed in the hexagon shown in Fig.2 corresponds to the limit of linear modulation. With (V/f) control, this operating condition would also correspond to the operation with rated frequency. From Fig. 2 it is evident that this operating condition corresponds to the case wherein the magnitude of the reference voltage space vector, denoted by $|\mathbf{v_{sr}}|$, is equal to $\sqrt{\frac{3}{2}}V_{dc}$. At any other magnitude of $|v_{sr}|$ lesser than $\sqrt{\frac{3}{2}}V_{dc}$, the frequency of the fundamental component is linearly related to the rated frequency.

The required DC-link voltage should be such that, the inverter outputs the rated peak phase voltage corresponding to the case when $|v_{sr}| = \sqrt{\frac{3}{2}}V_{dc}$. For an induction motor with a rated phase voltage of 230V (RMS), the peak voltage is 325V (i.e. $\sqrt{2}$ *230V).

Hence the required DC link voltage is given by:

$$\left(\frac{2}{3}\right)\sqrt{\frac{3}{2}}V_{dc} = 325 \text{ or } V_{dc} = 563\text{V} \quad (29)$$

In equation (29), the factor (2/3) arises from the fact that the length of the space vector is (3/2) times the peak of the individual phase voltages.
From the above discussion it is evident that the operating frequency (f_0) and the time period (T_0) of the fundamental component for a given modulation index are given by:

$$f_0 = \frac{v_{sr} * 50}{\left(\frac{\sqrt{3}}{2}\right) * V_{dc}} Hz \Rightarrow T_o = \frac{1}{f_o}$$

$$\text{i.e. } T_0 = \frac{\left(\frac{\sqrt{3}}{2}\right) * V_{dc}}{(v_{sr} * 50)} \quad (30)$$

As there are 48 samples per cycle, the time per one sample i.e. sampling time period (T_s) is given by:

$$T_s = \frac{T_o}{48} = \frac{\left(\frac{\sqrt{3}}{2}\right) * V_{dc}}{(|v_{sr}| * 50 * 48)} \quad (31)$$

A. *Experimental results with m_i =0.4 (40% modulation)*

The experimental waveform of the pole voltage (v_{AO}), the common-mode voltage content of the pole voltages (dropped across the AC-neutral point 'N' and the point 'O' in Fig. 1) and the phase voltage (v_{AN}) of the 3-phase two-level inverter operated in linear modulation (40% modulation) are shown in Fig. 5a, 5b and 5c respectively. The maximum phase voltage is given by $\frac{2}{3} * V_{dc}$ i.e. (0.667*563) = 376V.

The experimental results confirm this assertion, as is evident from Fig. 5. Fig. 6a shows the sample averaged 'T_{ga}' waveform applied to A-phase leg of the inverter for 40% modulation operation. It may be noted that it resembles that of the sample averaged pole voltage (v_{AO}). The time period of this waveform corresponds to the one given by equation 30. Substituting $|v_{sr}| = 0.4V_{dc}$ in eqn. 30, one gets T_o = 43.3 ms. The experimental result, reinforce this assertion. Fig. 6b shows the waveforms of v_α and v_β, corresponding to the case of linear-modulation. As one might expect, these waveforms are sinusoidal, phase shifted to each other by 90^0. Fig. 6c shows the locus of the tip of the reference vector in the $\alpha - \beta$ plane, corresponding to this case.

B. Experimental results for Over-modulation

The experimental waveform of the pole voltage (v_{AO}), the common-mode voltage content of the pole voltages (dropped across the AC-neutral point 'N' and the point 'O' in Fig. 1) and the phase voltage (v_{AN}) of the 3-phase two-level inverter corresponding to the case of over-modulation are shown in Fig. 7a, 7b and 7c respectively. Whenever the tip of the reference vector **OP** is situated outside the hexagon shown in Fig. 2, the imaginary switching times T_{as}, T_{bs} and T_{cs} are so adjusted as to bring the revised sample on to the periphery of the hexagon. Whenever it is detected that the null time duration $T_o < 0$, it is forced to zero and the values of the imaginary switching times are readjusted following the procedure described in [13]. In this case, the values to be loaded into the counters of the DSP are directly read from a *separate* lookup table, corresponding to the case of over-modulation. Fig. 8a shows the sample averaged 'T_{ga}' waveform applied to A-phase leg of the inverter for over-modulation. The inverter operates with a constant frequency of 50Hz, as the frequency is clamped to the rated frequency if the inverter operates in the region of over-modulation. Fig.8b shows the waveforms of v_α and v_β, corresponding to the case of over-modulation. As one might expect, these waveforms are non-sinusoidal, though they are phase shifted to each other by 90^0. Fig. 8c shows the locus of the tip of the reference vector in the $\alpha - \beta$ plane, corresponding to this case. The waveforms of v_a, v_β for a modulation index of 93% (i.e. $|v_{sr}| = 0.93V_{dc}$) are shown in Fig. 9a. In this case, the tip of the reference vector is partly situated within the hexagon shown in Fig. 2, resulting in the circular part of the locus and partly on the periphery of the hexagon. The samples situated within the hexagon are synthesized by switching two active vectors in the nearest proximity and two null vectors (with the redundancy of the null states) resulting in the circular part of the locus as $T_o > 0$ in this case. However, for the samples situated outside the hexagon, $T_o < 0$. Since it is impracticable to have a negative value for the switching period of the null vector, it is forced to zero filling the entire sampling time period with the effective time interval, T_{eff} [13]. This means that in the latter case, only the two active vectors situated in the nearest proximity to the tip of the reference vector. Thus, the tip of the reference vector is forced to lie in the periphery of the hexagon as demonstrated in Fig. 9b.

C. Advantage with the proposed corollary

As mentioned earlier, a corollary to the Kim-Sul algorithm for the implementation of space vector modulation is derived in this paper. This corollary is applicable for the case of under-modulation, when the induction motor is operated with v/f control. The proposed corollary is based on the observation that the imaginary switching times T_{as}, T_{bs} and T_{cs} remain unaltered for a given θ, even though the modulation index is varied in the aforementioned condition. Instead of computing the imaginary switching times T_{as}, T_{bs} and T_{cs} online, the corresponding values of T_{const} are computed offline and are stored in a lookup table (Table-1 for an easy reference). To this value, the value of $T_s/2$ is either added or subtracted, depending on the sequence to be implemented to directly generate the gating waveforms of the individual devices. For over-modulation, a separate lookup table is employed (Table-2), with the amendment suggested in [13]. In other words, if the sample is situated within the hexagon shown in Fig. 2, the inverter leg switching timings T_{ga}, T_{gb} and T_{gc} are computed using T_{const} obtained by reading off Table-1, while they are read off the Table-2, if they are situated outside the hexagon. Fig. 10 shows the reduction in the time of computation with the proposed modification. To discern the difference clearly, the computation time is increased by a factor of eight by introducing 8 wait states between each instruction of the interrupt subroutine. The time period between each interrupt is equal to the sampling time period. The time periods for a given sample are computed one sampling time period ahead, i.e. the periods calculated in the current sampling time are implemented in the subsequent sampling time interval. The upper trace of Fig. 10 shows the time of computation with the proposed corollary, while the lower trace shows the time of computation with the conventional Kim-Sul algorithm. From the top trace, it may be noted that the time of computation is 50μs with the proposed modification, while it is about 80μs with the conventional Kim-Sul algorithm. This means that the actual times of computation are $1/8^{th}$ of these timings as 8 wait states are deliberately introduced between each instruction to measure these time periods accurately. The experimental condition corresponds to the modulation index of 0.8, for which the sampling time period is 451μs (eqn.31). From the above figure it is evident the computation has become faster by a factor of (80-50)/80, i.e. by about 37%.

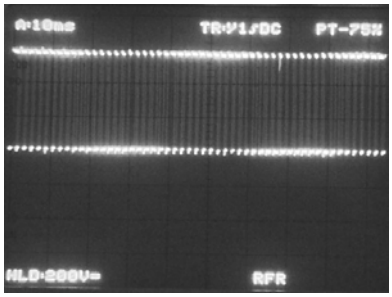

Fig. 5a: Experimental waveform of the pole voltage (Scale: time axis: 10ms/div, Voltage axis: 200V/div.)

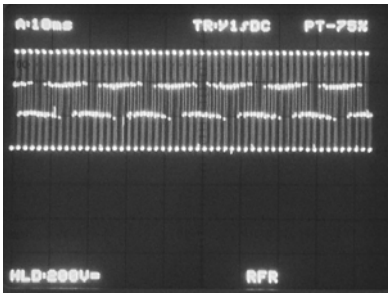

Fig. 5b: Waveform of the common-mode voltage (Scale: time axis: 10ms/div and Voltage axis: 200Vdiv.)

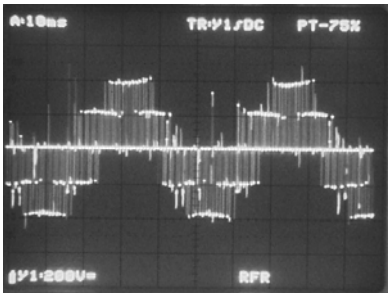

Fig. 5c: Experimental waveform of the phase voltage (time: 10ms/div and Voltage: 200V/div.)

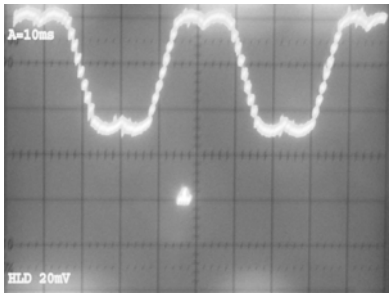

Fig. 6a: The waveform of sample averaged T_{ga} at a modulation index of 40% (Time axis: 10ms / div.)

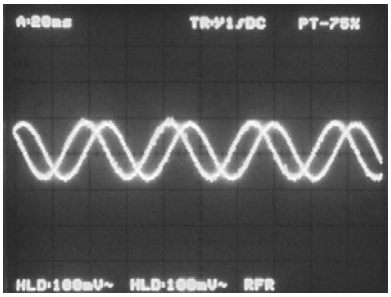

Fig. 6b: The waveforms of v_a and v_β at a modulation index of 40% (Time axis: 20ms / div.)

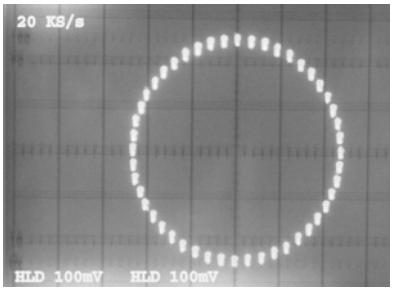

Fig. 6c: The locus of the tip of the reference vector at a modulation index of 40%

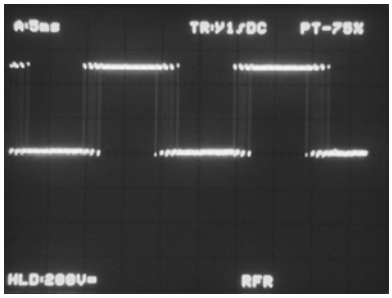

Fig. 7a: Waveform of the pole voltage for over-modulation (Scale: time axis: 5ms/div and Voltage axis: 200V/div.)

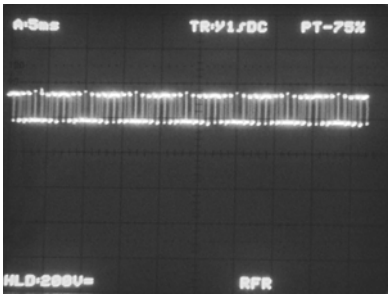

Fig. 7b: Waveform of the common-mode voltage for over-modulation (Scale: time axis: 5ms/div and Voltage axis: 200V/div.)

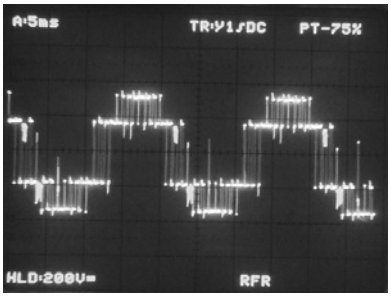

Fig. 7c: Waveform of the phase voltage for over-modulation (Scale: time axis: 5ms/div and Voltage axis: 200V/div.)

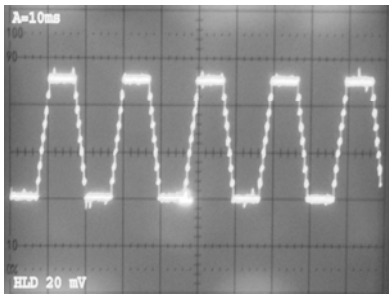

Fig. 8a: The waveform of sample averaged T_{ga} for over- modulation (Time axis: 10ms / div.)

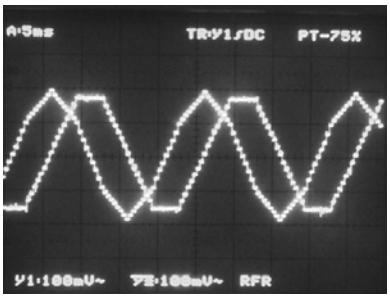

Fig. 8b: The waveforms of v_a and v_β for over-modulation (Time axis: 5ms / div.)

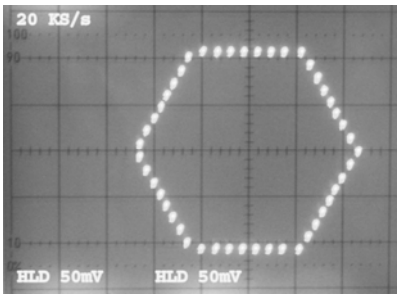

Fig. 8c: The locus of the tip of the reference vector for over-modulation

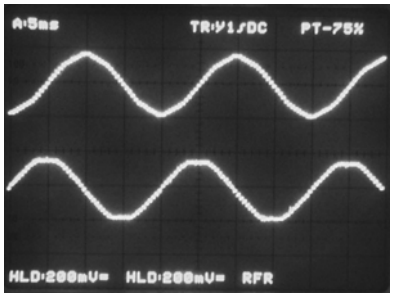

Fig. 9a: The waveforms of v_α and v_β at a modulation index of 93% (x-axis: 5ms /div)

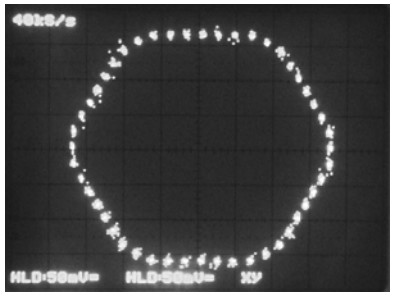

Fig. 9b: The locus of the tip of the reference vector at a modulation index of 93%

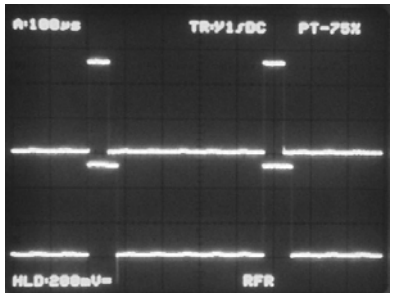

Fig. 10: The time of execution with the proposed corollary (upper trace) and with the conventional algorithm (lower) (Time scale: 100µs/div)

V. Conclusion

In this paper, a corollary to the Kim-Sul algorithm is derived, which is useful in implementing the synchronized SVM for a 3-phase, 2-level inverter driving an induction motor with (V/f) control. This corollary reduces the computational overhead on the digital controller by about 37%. An elegant lookup table is devised, which could be used for any modulation index, while the inverter is operated within the range of modulation. The Kim-Sul algorithm with this corollary is experimentally implemented on a TMS320F243 DSP platform. The experimental results validate the proposed corollary to the Kim-Sul algorithm.

References

[1] Jacob Zubek, Alberto Abbondanti and Craig J. Norby, "Pulsewidth modulated inverter motor drives with improved modulation", IEEE Trans. Ind. Applicat., Vol.IA-11, No.6 Nov/Dec 1975, pp. 695-703.

[2] R.M. Green and J.T.Boys, "Implementation of pulsewidth modulated inverter modulation strategies", IEEE Trans. Ind. Applicat., Vol.IA-18, No.2 Mar/Jun 1982, pp. 138-145.

[3] Alberto Pollmann, "A digital pulse width modulator employing advanced modulation techniques", IEEE Trans. Ind. Applicat., Vol.IA-19, No.3, May/Jun. 1983, pp.409-414.

[4] Heinz Willi Van Der Broeck, Hans-Christopher Skudenly and Georg Viktor Stanke, "Analysis and realization of a pulsewidth modulator based on voltage space vectors", IEEE Trans. Ind. Applicat., Vol.24, No.1 Jan/Feb. 1988, pp.142-150.

[5] Ned Mohan, Tore M.Undeland, William P. Robbins, "Power Electronics: Converters, Applications and Design", (John Wiley& Sons, Second Edition, 1995).

[6] Sidney R Bowes and Yen-Shin Lai, "The relation between space-vector modulation and regular-sampled PWM", IEEE Trans. Ind. Applicat., Vol.44, No.5 Oct 1997, pp.670-679.

[7] Donald Grahame Holmes, "The significance of zero space vector placement for carrier-based PWM schemes", IEEE Trans. Ind. Applicat., Vol.32, No.5 Sept/Oct 1996, pp.1122-1129.

[8] Keliang Zhou and Danwei Wang, "Relationship between space vector modulation and three phase carrier-based PWM: A comprehensive analysis", IEEE Trans. Ind. Applicat., Vol.49, No.1, Feb 2002, pp.186-196.

[9] Joachim Holtz, "Pulsewidth modulation- a survey", IEEE Trans. Ind. Applicat., Vol.39, No.5, Dec 1992, pp.410-420.

[10] V. Oleschuk and F. Blaabjerg, "Direct synchronized PWM techniques with linear control functions for adjustable speed drives", in Proc. of the IEEE APEC'2002, pp.76-82.

[11] V. Oleschuk, F. Blaabjerg and B.K. Bose, "Triphase cascaded converters with direct synchronous pulsewidth modulation", Automatica, Vol.44, No.1-2, pp.27-33, 2003.

[12] Narayanan, G., Krishnamurthy, H.K., Di Zhao and Ayyanar, R. "Advanced bus-clamping PWM techniques based on space vector approach" IEEE Tran. Power Electronics, Vol.21, No. 4, July '06, pp. 974-984.

[13] Joohn-Sheok Kim, Seung-Ki Sul, "A novel voltage modulation technique of the space vector PWM, Conf. Proc.IPEC- 1995, pp.742-747.

Biographies

K.A.S.Mallikarjuna Rao received his B.Tech. degree in Electrical Engineering from the National Institute of Technology, Warangal, India in 2004 and the M.E. degree in Power Electronics at Indian Institute of Science (IISc), Bangalore, India in 2007. He is presently working as a Senior Engineer in M/S Ashok Leyland Ltd, Chennai, India. His areas of interest include Power Electronics, Motor Drives and PWM techniques.

Sunita Nadampalli received her B.Tech. degree from the National institute of Technology, Warangal, India in 2005 in Electrical Engineering. She is the winner of six gold medals for her academic excellence. She is currently working as a Software Design Engineer at M/s Texas Instruments (India) Ltd, Bangalore, India.

V.T. Somasekhar received his graduate degree from Regional Engineering College Warangal (presently the National Institute of Technology) in 1988 and the post graduate degree from the Indian Institute of Technology, Bombay in 1990, his area of specialization being Power Electronics. He received his doctoral degree from the Indian Institute of Science in 2003. His current interests are multilevel inversion with open-end induction motors, AC drives and PWM strategies.